BBA - Molecular Basis of Disease 1865 (2019) 2671–2684

Contents lists available at ScienceDirect

BBA - Molecular Basis of Disease

journal homepage: www.elsevier.com/locate/bbadis

The adipokine sFRP4 induces insulin resistance and lipogenesis in the liver

Tina Hörbelt[a,b,c,1], Birgit Knebel[a,b,1], Pia Fahlbusch[a,b,c], David Barbosa[a,b,c], Daniella Herzfeld de Wiza[a,b], Frederique Van de Velde[d], Yves Van Nieuwenhove[e], Bruno Lapauw[d], G. Hege Thoresen[f,g], Hadi Al-Hasani[a,b,c], Dirk Müller-Wieland[h], D. Margriet Ouwens[a,b,d,1], Jorg Kotzka[a,b,*,1]

[a] Institute of Clinical Biochemistry and Pathobiochemistry, German Diabetes Center at the Heinrich-Heine-University Duesseldorf, Leibniz Center for Diabetes Research, Auf'm Hennekamp 65, 40225 Duesseldorf, Germany
[b] German Center of Diabetes Research Partner, Duesseldorf, Germany
[c] Medical Faculty, Institute for Clinical Biochemistry and Pathobiochemistry, German Diabetes Center (DDZ), Heinrich Heine University, Düsseldorf, Germany
[d] Department of Endocrinology, Ghent University Hospital, Ghent, Belgium
[e] Department of Gastrointestinal Surgery, Ghent University Hospital, Ghent, Belgium
[f] Section for Pharmacology and Pharmaceutical Biosciences, Department of Pharmacy, University of Oslo, Oslo, Norway
[g] Department of Pharmacology, Institute of Clinical Medicine, University of Oslo, Oslo, Norway
[h] Clinical Research Centre, Department of Internal Medicine I, University Hospital Aachen, Aachen, Germany

ARTICLE INFO

Keywords:
Insulin action
Adipokines
NAFLD
Insulin resistance
Hepatic insulin resistance
sFRP4
FoxO1

ABSTRACT

Secreted frizzled-related protein (sFRP) 4 is an adipokine with increased expression in white adipose tissue from obese subjects with type 2 diabetes and non-alcoholic fatty liver disease (NAFLD). Yet, it is unknown whether sFRP4 action contributes to the development of these pathologies. Here, we determined whether sFRP4 expression in visceral fat associates with NAFLD and whether it directly interferes with insulin action and lipid and glucose metabolism in primary hepatocytes and myotubes. The association of sFRP4 with clinical measures was investigated in obese men with or without type 2 diabetes and with or without biopsy-proven NAFLD. To determine the impact of sFRP4 on metabolic parameters, primary human myotubes (hSkMC), or primary hepatocytes from metabolic healthy C57Bl6 and from systemic insulin-resistant mice, i.e. aP2-SREBP-1c, were used. Gene expression of *sFRP4* in visceral fat from obese men associated with insulin sensitivity, triglycerides and NAFLD. In C57Bl6 hepatocytes, sFRP4 disturbed insulin action. Specifically, sFRP4 decreased the abundance of IRS1 and FoxO1 together with impaired insulin-mediated activation of Akt-signalling and glycogen synthesis and a reduced suppression of gluconeogenesis by insulin. Moreover, sFRP4 enhanced insulin-stimulated hepatic de novo lipogenesis (DNL). In hSkMC, sFRP4 induced glycolysis rather than inhibiting insulin signalling. Finally, in hepatocytes from aP2-SREBP-1c mice, sFRP4 potentiates existing insulin resistance. Collectively, we show that sFRP4 interferes with hepatocyte insulin action. Physiologically, sFRP4 promotes DNL in hepatocytes and glycolysis in myotubes. These sFRP4-mediated responses may result in a vicious cycle, in which enhanced rates of DNL and glycolysis aggravate hepatic lipid accumulation and insulin resistance.

1. Introduction

In obesity, the adipose tissue expands due to an enhanced storage of lipids in white adipocytes. Yet, an impaired lipid storage capacity of the adipose tissue contributes to increased lipid deposition in non-adipose tissues, including the liver. Ectopic lipid distribution may result from excess caloric intake resulting in obesity, but also characterizes disorders associated with impaired lipid storage capacity, such as lipodystrophies [1]. Obesity alters the secretion of hormones, called adipokines, from adipose tissue and alterations in adipokine secretion have

Abbreviations: ALT, alanine aminotransferase; BMI, body mass index; BZ, bortezomib; DNL, de novo lipogenesis; GGT, gamma-glutamyl transferase; HOMA-IR, homeostatic model assessment of insulin resistance; HOMA2-%B, homeostatic model assessment of beta cell function; NAFLD, non-alcoholic fatty liver disease; SAT, subcutaneous adipose tissue; sFRP4, secreted frizzled-related protein; SREBP-1c, sterol-regulatory element binding protein-1c; VAT, visceral adipose tissue

* Corresponding author at: Institute of Clinical Biochemistry and Pathobiochemistry, German Diabetes Center, Heinrich-Heine-University Duesseldorf, Leibniz Center for Diabetes Research, Aufm Hennekamp 65, 40225 Duesseldorf, Germany.
E-mail address: joerg.kotzka@ddz.de (J. Kotzka).
[1] Both authors contributed equally.

https://doi.org/10.1016/j.bbadis.2019.07.008
Received 22 March 2019; Received in revised form 19 June 2019; Accepted 18 July 2019
Available online 20 July 2019
0925-4439/

been linked to the inhibition of insulin action in peripheral tissues like the liver and skeletal muscle, but also to the development of diabetes-associated complications like non-alcoholic fatty liver disease (NAFLD) [2].

The prevalence of NAFLD is rapidly increasing along with the pandemic increase in obesity [3]. The first step in the development of NAFLD is lipid accumulation in hepatocytes. This increase in intracellular lipids may result from higher rates of de novo lipogenesis (DNL), a raised flux of fatty acids from adipose tissue to the liver and a higher uptake of dietary lipids [4]. Clinical studies indicate that NAFLD is strongly associated with hepatic insulin resistance and type 2 diabetes [5]. When hepatic steatosis is accompanied by tissue inflammation, necrosis and fibrosis, the disease proceeds from the more severe non-alcoholic steatohepatitis to end-stage liver disease [6,7].

There is currently limited understanding on the importance of adipokines for the development of NAFLD. Secreted frizzled-related protein (sFRP) 4, a member of regulators of the Wingless-type (Wnt) signalling pathway activity, is one of the adipokines showing an altered expression and secretion from visceral adipose tissue (VAT) in obesity and from patients with NAFLD [8–10]. Furthermore, circulating levels of sFRP4 are increased in obesity and type 2 diabetes and associated with the development of β-cell dysfunction [8,9]. Whereas in vitro studies show direct effects of sFRP4 on insulin secretion by β-cells, little is known on metabolic effects of sFRP4 in target tissues for insulin action, such as the liver. Based on the increased expression of sFRP4 in VAT from patients with NAFLD [10], and its association with insulin resistance [8,11], we hypothesize that sFRP4 impacts on the liver by interfering with insulin action and hepatic glucose and lipid metabolism. This was examined in primary hepatocytes from metabolically healthy C57Bl6 mice and from mice with systemic insulin resistance and lipodystrophy, namely the aP2-SREBP-1c model [12,13]. Furthermore, we examined sFRP4 action in primary human myotubes.

2. Materials and methods

2.1. Study participants

We examined 36 normal-weight and 109 obese men from the previously described Obster and HepObster study conducted at the Ghent University hospital according of the Declaration of Helsinki (Clinical Trials Registration numbers NCT00740194 and B67020084018) [10,14,15]. The study protocol was approved by the Ethics Committee of Ghent University Hospital and participants gave written informed consent. During surgery, biopsies from subcutaneous and visceral adipose tissue were collected from the abdominal region, immediately snap frozen in liquid nitrogen and stored at −80 °C for gene expression analysis as described [10]. In addition, a liver biopsy was obtained from 54 obese participants, which was used for histological examination of steatosis, lobular inflammation, ballooning and fibrosis as described previously [10]. The histological data were used to calculate the steatosis, activity and fibrosis score, which discriminates between NAFLD and NASH [16], and the NAFLD activity score [7]. Overnight fasting blood samples were collected prior to surgery for analysis of sFRP4, and clinical measures as described [10,15]. HOMA-IR was calculated as (fasting glucose [mmol/L] × (fasting insulin [μU/mL])/22.5)), and HOMA2-%B was calculated as (20 × fasting insulin [μU/ml])/(glucose [mmol/l]-3.5).

2.2. Experimental animals

The animal experiments were approved by the Animal Care Committee of the University Düsseldorf (approval number Az.84-02.04.2015.A424, 2015), and performed according to the 'Principle of laboratory animal care' (NIH publication No. 85-23, revised 1996) and the German law on the protection of animals. We used male C57Bl6 and transgenic mice that overexpress the transcriptional active form of human SREBP-1c (aa 1–436) under the control of the adipocyte-specific aP2 enhancer/promoter that were backcrossed on C57Bl6 for > 20 generations aged between 18 and 24 weeks [12,13]. Mouse sFRP4 plasma levels were determined using a mouse sfrp4 ELISA kit (BIOZOL, Eching, Germany) according to manufacturer's recommendations.

2.3. Isolation and culture of primary murine hepatocytes

Primary hepatocytes were isolated by a two-step collagenase perfusion protocol as described [13], and used within 24 h after isolation.

2.4. Culture of primary skeletal muscle cells

Primary human skeletal muscle cells were differentiated from commercially available proliferating satellite cells (Lonza, Basel Switzerland) as described [14]. Cells from at least four different male and female healthy Caucasian donors aged between 16 and 41 years were used.

2.5. Cell culture treatment

For signalling experiments, cell cultures were serum-starved for 4 h prior to a 24 h incubation with 100 μg/l sFRP4 (R&D Systems, Wiesbaden, Germany). This concentration was based on the circulating levels in obese men [10]. When indicated, the cultures were incubated with 10 nmol/l bortezomib (Merck, Darmstadt, Germany) for 30 min prior to sFRP4 addition, or with 100 nmol/l insulin (Sigma-Aldrich, Taufkirchen, Germany) for additional 10 min. In gluconeogenesis experiments, hepatocytes were serum-starved for 20 h. For glycogen synthesis, hepatocytes were glucose-starved for 90 min prior to the assay.

2.6. RNA extraction and analysis of gene expression

The quantification of *sFRP4* gene expression in human VAT and SAT was described [10]. Gene expression in murine adipose tissue, liver, pancreas and m. *gastrocnemius*, and hepatocytes, was quantitated by real-time PCR using gene-specific assays for acetyl-CoA carbocylase α (*Acaca*), acyl-CoA thioesterase 2 (*Acot2*), carnitine palmitoyltransferase 1a (*Cpt1a*), carnitine palmitoyltransferase 2 (*Cpt2*), fatty acid synthase (*Fasn*), Foxo1, Glucose-6-phosphatase, catalytic subunit (*G6Pc*), hepatic nuclear factor 4α (*Hnf4a*), malic enzyme 1 (*Me1*), Mlx interacting protein-like (*Mlxipl,* also known as carbohydrate-response element binding protein 1, *ChREBP*), phosphoenolpyruvate carboxykinase 1 *(Pck1)*, peroxisome proliferator activated receptor α (*Ppara*), ribosomal protein S18 *(RPS18)*, *sFRP4* and sterol regulatory element-binding transcription factor 1 (*Srebp1c*) (Thermofisher, Darmstadt, Germany) as described [17].

2.7. Analysis of insulin action

The phosphorylation and abundance of components of insulin action was examined by Western blotting as described elsewhere [14].

2.8. Analysis of sirtuin activity

Sirtuin (SIRT) activity was examined in cell lysates (5 μg protein) using a luminescence-based SIRT-Glo™ assay system (Promega, Mannheim, Germany) according to manufacturer's instructions.

2.9. Glycogen synthesis

Glycogen synthesis was determined by the incorporation of D-[^{14}C(U)]-glucose into glycogen as described [14].

Table 1
Patient characteristics.

Variable	Normal weight	Obese	Obese + type 2 diabetes	P
N	36	58	51	
Age, years	48.2 ± 13.6	42.1 ± 11.1*	52.2 ± 9.9†††	< 0.001
BMI, kg^2/m	24.0 ± 2.76	41.2 ± 5.47***	43.1 ± 6.88***	< 0.001
HbA1c, %	n.a.	5.78 ± 0.43	7.31 ± 1.66††	0.009
Fasting glucose, mmol/l	4.83 (4.31–5.58)	5.33 (4.77–5.85)	7.00 (6.21–9.24)***,†††	< 0.001
Fasting insulin, pmol/l	31.7 (21.0–43.5)	90.3 (55.8–163)**	135 (83.7–226)***	< 0.001
HOMA-IR	0.89 (0.63–1.53)	2.96 (1.72–5.37)	n.a.	0.011
HOMA2%B	67.5 (45.1–104)	118 (79.3–182)	n.a.	< 0.001
ALT, IU/l	23.0 (15.0–36.0)	48.0 (35.5–67.5)**	45.0 (27.0–63.0)**	< 0.001
AST, IU/L	20.0 (15.0–36.0)	28.0 (24.0–37.0)	32.0 (23.0–41.0)**	0.005
γGT, IU/L	25.0 (14.0–35.0)	40.0 (31.5–56.0)*	39.0 (24.0–62.0)**	0.003
TG, mg/dl	133 (90.0–185)	175 (131–268)	161 (131–245)	0.037

The data are presented as mean ± SD in case of normally distributed datasets or as median (interquartile range) in case of skewed datasets. Differences between the participant groups were calculated using ANOVA and Bonferroni correction for multiple comparisons.
BMI, body mass index; HOMA-IR, Homeostatic model assessment of insulin resistance; HOMA2%B Homeostatic model assessment of beta cell function; ALT, alanine amino transferase; AST, aspartate aminotransferase; γGT, gamma glutamyl transferase; TG, triglycerides.
*** Indicate $p < 0.001$ for differences versus normal weight control men.
** Indicate $p < 0.01$ for differences versus normal weight control men.
* Indicate $p < 0.05$ for differences versus normal weight control men.
††† Indicates $p < 0.001$ for differences between obese men with and without type 2 diabetes.
†† Indicates $p < 0.01$ for differences between obese men with and without type 2 diabetes.

2.10. Gluconeogenesis

Glucose production in hepatocytes was determined by quantification of the amount of glucose in the supernatant after the various treatments as described [14]. Expression of *G6pc* and *Pck1* was examined by real-time PCR as described under 2.6.

Determinants of mitochondrial function and glycolysis were examined using a Seahorse extracellular flux analyser (Agilent Technologies, Waldbronn, Germany). Mitochondrial function in hepatocytes was determined using the mito-stress as described [18]. In primary myotubes, the mito-stress test was performed in the presence of 150 µmol/l palmitate coupled to BSA or the equivalent amount of BSA [18]. Glycolysis was analyzed in myotubes using the glycolytic rate assay [19]. The WAVE software (Agilent Technologies, version 2.6.0) was used to calculate determinants of glycolysis and mitochondrial function.

2.11. Fatty acid oxidation

Fatty acid oxidation was examined in primary hepatocytes and myotubes by quantifying oxidation of [^{14}C]-palmitate into $^{14}CO_2$. The $^{14}CO_2$ release was normalized to protein content presenting fatty acid oxidation [19].

2.12. Analysis of cellular fatty acid uptake

Fatty acid uptake in skeletal muscle cells and primary hepatocytes was detected as described [13,14,20].

2.13. De novo lipogenesis (DNL) in primary hepatocytes

The impact of sFRP4 on DNL in primary hepatocytes was determined by the incorporation of ^{14}C-acetate into lipids as described [14].

2.14. Statistical analysis

Clinical study data were analyzed using SPSS Statistics (v25.0; IBM, Armonk, NY, USA). The other data were analyzed with GraphPad Prism (v7.04, GraphPad software, LaJolla, CA, USA). All data are expressed as mean (95% CI) unless indicated otherwise. Differences between two groups were calculated by Student *t*-test. In case of more groups, differences were calculated by one- or two-way ANOVA followed by Sidak correction for multiple comparisons. Variables with a skewed distribution were log-transformed prior to linear regression analysis with adjustments for age and/or BMI. A *p*-value of 0.05 was considered as statistically significant.

2.15. Key resources table

Resource	Source	Identifier
Chemical		
[14C] -palmitate		
14C- acetate		
acetyl-CoA		
bortezomib		
carbohydrate		
Fatty acid		
Glucose		
palmitate		
ProteinPeptide		
insulin		
IR		
sfrp4		
SREBP-1c		
sterol regulatory element-binding transcription factor 1		

3. Results

3.1. sFRP4 serum levels and gene expression in adipose tissue in obesity and type 2 diabetes

We examined circulating sFRP4 levels and adipose tissue mRNA levels in samples from a previously described clinical study on normal-weight and obese men [14]. The characteristics of the study participants (normal-weight: n = 36; obese: n = 109, including n = 51 with type 2 diabetes) are summarized in Table 1. The obese men had a higher body mass index (BMI), fasting insulin, alanine aminotransferase (ALT) and gamma-glutamyl transferase (GGT) levels, and were insulin resistant as estimated by homeostatic model assessment (HOMA-IR) (all $p < 0.001$; except for GGT, $p = 0.01$) versus normal-weight men. The obese men with type 2 diabetes were older versus the participants without type 2 diabetes ($p < 0.001$), and had higher Hb1Ac ($p < 0.01$) and fasting glucose levels ($p < 0.001$).

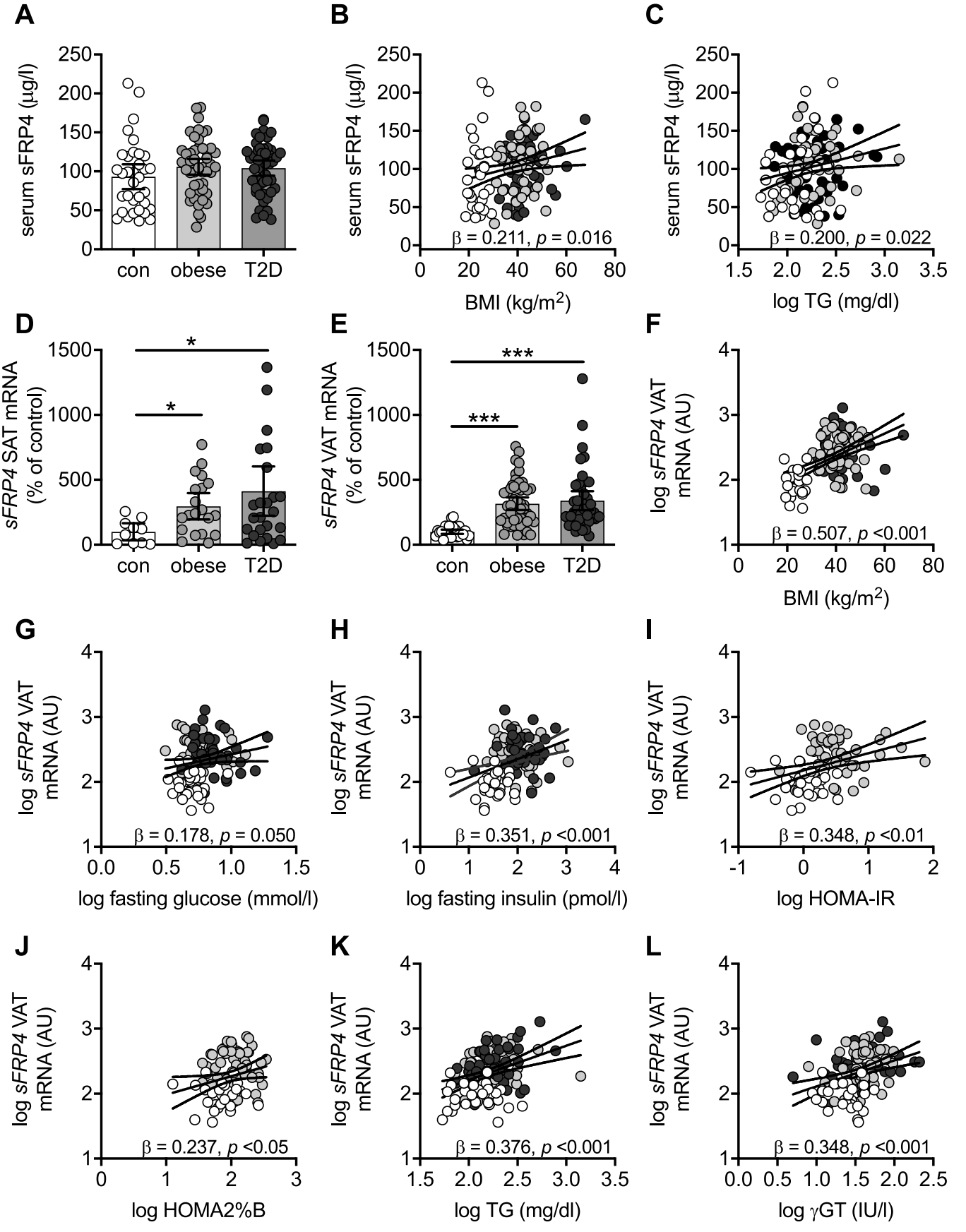

(caption on next page)

Fig. 1. Serum sFRP4 levels and expression in human subcutaneous and visceral adipose tissue.
(A) Circulating serum sFRP4 levels from normal weight (control, n = 34) and obese men with (n = 48) and without (n = 50) type 2 diabetes (T2D). Data are expressed as dot plots showing the mean and 95% CI for each group. Differences among the groups were analyzed by ANOVA and Sidak's correction for multiple comparisons.
(B,C) The graphs depict the regression lines and 95% confidence bands (dotted lines). The open dots represent normal weight men, the grey dots represent obese men without T2D, and filled dots obese men with T2D.
(D, E) Gene expression of sFRP4 in SAT (a) and VAT (b) from normal weight (control, n = 13 [a], n = 28 [b]) and obese men with (n = 24 [a], n = 43 [b]) and without type 2 diabetes (T2D) (n = 20 [a], n = 51 [b]). Data are expressed as dot plots showing the mean and 95% CI for each group. Differences among the groups were analyzed by ANOVA and Sidak's correction for multiple comparisons. ***, $p < 0.001$ versus control. (F–L) Correlates between *sFRP4* expression in VAT and BMI (F), fasting glucose (G), fasting insulin (H), HOMA-IR (I), HOMA-2%B (J), triglycerides (K), and γGT (L). The standardized regression coefficient β and *p*-values were calculated using linear regression analysis for the entire cohort. The graphs depict the regression lines and 95% confidence bands (dotted lines). The open dots represent normal weight men, the grey dots represent obese men without T2D, and filled dots obese men with T2D.

3.2. Correlates of sFRP4 serum and gene expression levels

Although we observed no statistically significant differences in circulating sFRP4 levels among the three groups (Fig. 1A), sFRP4 in serum associated with BMI ($r = 0.211$, $p < 0.05$) and triglycerides ($r = 0.200$, $p < 0.05$) (Supplementary Tables 1, 2, Fig. 1B–C). In SAT, sFRP4 mRNA was increased by 3.0- and 4.1-fold in biopsies from obese men without and with type 2 diabetes, respectively (both $p < 0.05$ versus control) (Fig. 1D), and SAT *SFRP4* mRNA levels associated with BMI ($r = 0.267$, $p < 0.05$), fasting insulin ($r = 0.320$, $p < 0.05$), HOMA2%B ($r = 0.362$, $p < 0.05$), and triglycerides ($r = 0.433$, $p < 0.001$) (Supplementary Fig. 1).

In VAT, *sFRP4* mRNA was increased by 3.2- and 3.4-fold in biopsies from obese men without and with type 2 diabetes, respectively (both $p < 0.001$ versus control) (Fig. 1E). VAT expression of *sFRP4* correlated with BMI ($r = 0.507$, $p < 0.01$), fasting insulin ($r = 0.351$, $p < 0.01$), HOMA-IR ($r = 0.348$, $p < 0.01$), HOMA2%B ($r = 0.237$, $p < 0.01$), and triglycerides ($r = 0.376$, $p < 0.01$). Furthermore, associations were found for ALT ($r = 0.277$, $p < 0.01$) and GGT ($r = 0.348$, $p < 0.01$) (Fig. 1F–L). Adjusting for age had no profound impact, whereas only the associations of VAT *sFRP4* mRNA and GGT ($\beta = 0.231$, $p < 0.01$) and triglycerides ($\beta = 0.255$, $p < 0.01$) remained robust upon additional correction for BMI (Supplementary Tables 1, 2).

When stratifying the cohort according to fatty liver disease state, *sFRP4* mRNA abundance in VAT was increased by 2.7- and 3.3-fold in biopsies from men with NALFD and NASH, respectively (Supplementary Fig. 2A) (both $p < 0.001$). Furthermore, *sFRP4* expression associated with the NAFLD activity score (Supplementary Fig. 2B) ($r = 0.509$, $p < 0.001$). Histological analysis further revealed that sFRP4 expression was increased upon the presence of the defining component of NAFLD, namely steatosis, lobular inflammation, ballooning, or fibrosis (Supplementary Fig. 2C–F).

3.3. sFRP4 impairs hepatic insulin action

Since the clinical data suggest that sFRP4 may interfere with insulin action as well as hepatic lipid- and glucose metabolism, we first examined the effects of recombinant sFRP4 on insulin action in primary murine hepatocytes isolated from metabolically healthy C57Bl6 mice. Pre-incubation with sFRP4 impaired the insulin-mediated phosphorylation of Akt-Ser473 by 46% ($p < 0.01$) (Fig. 2A), but had no significant inhibitory effect on insulin-mediated Akt-Thr308 phosphorylation (Fig. 2B). Furthermore, sFRP4 completely blocked the induction of the insulin-mediated phosphorylation of the Akt-targets GSK3β-Ser9 and FoxO1-Ser256 (Fig. 2C–D). These effects of sFRP4 on insulin action were not accompanied by changes in the basal phosphorylation of Akt-Thr473, GSK3β-Ser9 and FoxO1-Ser256 or in the protein abundances of Akt and GSK3β (Fig. 2A–C). However, sFRP4 incubation reduced the protein abundance of FoxO1 by 55% ($p < 0.001$) (Fig. 2E). The lower FoxO1 protein abundance suggests that sFRP4 suppresses the expression of FoxO1-regulated genes. Yet, besides phosphorylation, which promotes nuclear exclusion of the protein, FoxO1-activity is regulated by acetylation, and the SIRT-mediated deacetylation of FoxO1 increases the DNA binding affinity and activity of the protein [21]. Treatment with sFRP4 was found to reduce SIRT activity by 40% ($p < 0.05$) in C57Bl6 hepatocytes (Fig. 2F), further supporting the notion that sFRP4 inhibits the expression of FoxO1-target genes.

More upstream in the insulin signalling cascade, we found that the protein level of IRS2, a key regulator of the insulin signalling cascade, was not affected by sFRP4 (Fig. 2G). Yet, IRS1 protein abundance was reduced by 35% ($p < 0.001$) in hepatocytes treated with sFRP4 versus untreated cells (Fig. 2H). *Irs1* mRNA expression was not altered (Fig. 2I). The sFRP4-mediated post-translational reduction in IRS1 protein abundance was absent when the cells were pre-treated with the proteasome inhibitor bortezomib (BZ) (Fig. 3A). BZ alone had no effect on IRS1 abundance (Fig. 3A). Furthermore, sFRP4 did not inhibit insulin-mediated Akt-Ser473 and GSK3β-Ser9 phosphorylation in hepatocytes treated with BZ (Fig. 3B and C). However, BZ did not restore FoxO1 protein abundance and inhibition of insulin-mediated FoxO1-Ser256 phosphorylation in sFRP4-treated hepatocytes (Fig. 3D and E).

3.4. Effects of sFRP4 on hepatic glucose and lipid metabolism

The gluconeogenic substrates pyruvate and lactate increased glucose production by 1.5-fold versus untreated hepatocytes ($p < 0.001$) (Fig. 4A). Insulin suppressed glucose production by 1.2-fold in the presence of lactate and pyruvate (Fig. 4A). This insulin-mediated suppression of substrate-induced glucose production was not observed in hepatocytes exposed to sFRP4 (Fig. 4A). Insulin-mediated glycogen synthesis was lower in hepatocytes exposed to sFRP4 prior to insulin stimulation ($p < 0.05$) (Fig. 4B). Furthermore, insulin suppressed the mRNA levels of Pck1 and G6pc by 1.7-fold ($p < 0.05$) and 2.2-fold ($p < 0.01$), respectively (Fig. 4C and D). Incubating hepatocytes with sFRP4 lowered G6pc expression by 40% ($p < 0.05$) (Fig. 5C). Moreover, sFRP4 treatment abrogated the reduction of Pck1 and G6pc mRNA levels by insulin (Fig. 4C and D). This was not the case for the stimulation of DNL by insulin. Insulin promoted acetate incorporation into lipids by 1.5-fold in hepatocytes, and sFRP4 incubation enhanced this further by 1.5-fold in an additive way ($p < 0.05$) (Fig. 4E). In line with this observation, insulin and sFRP4 increased the mRNA levels of fatty acid synthase (*Fasn*) by 2.7-fold ($p < 0.001$) and 2.5-fold ($p < 0.01$), respectively, whereas an additive 5.0-fold increase in *Fasn* mRNA levels ($p < 0.001$) was observed after combined sFRP4 and insulin treatment (Supplementary Fig. 3). Exposing hepatocytes to sFRP4 only had no effect on the gene expression of other regulators of fatty acid metabolism, such as the transcription factors *Foxo1, Hnf4a, MlxipI, Ppara, Srebp1c*, and the catabolic enzymes *Acaca, Acot2, Cpt1a, Cpt2*, and *Me1* (Supplementary Fig. 3). Insulin was found to increase the mRNA levels *Cpt1, Foxo1, Hnf4a,* and *MlxipI*, and this was not observed when hepatocytes were exposed to sFRP4 prior to insulin treatment (Supplementary Fig. 3).

3.5. Effects of sFRP4 on hepatic mitochondrial function

The afore-mentioned data show that sFRP4 promotes de novo

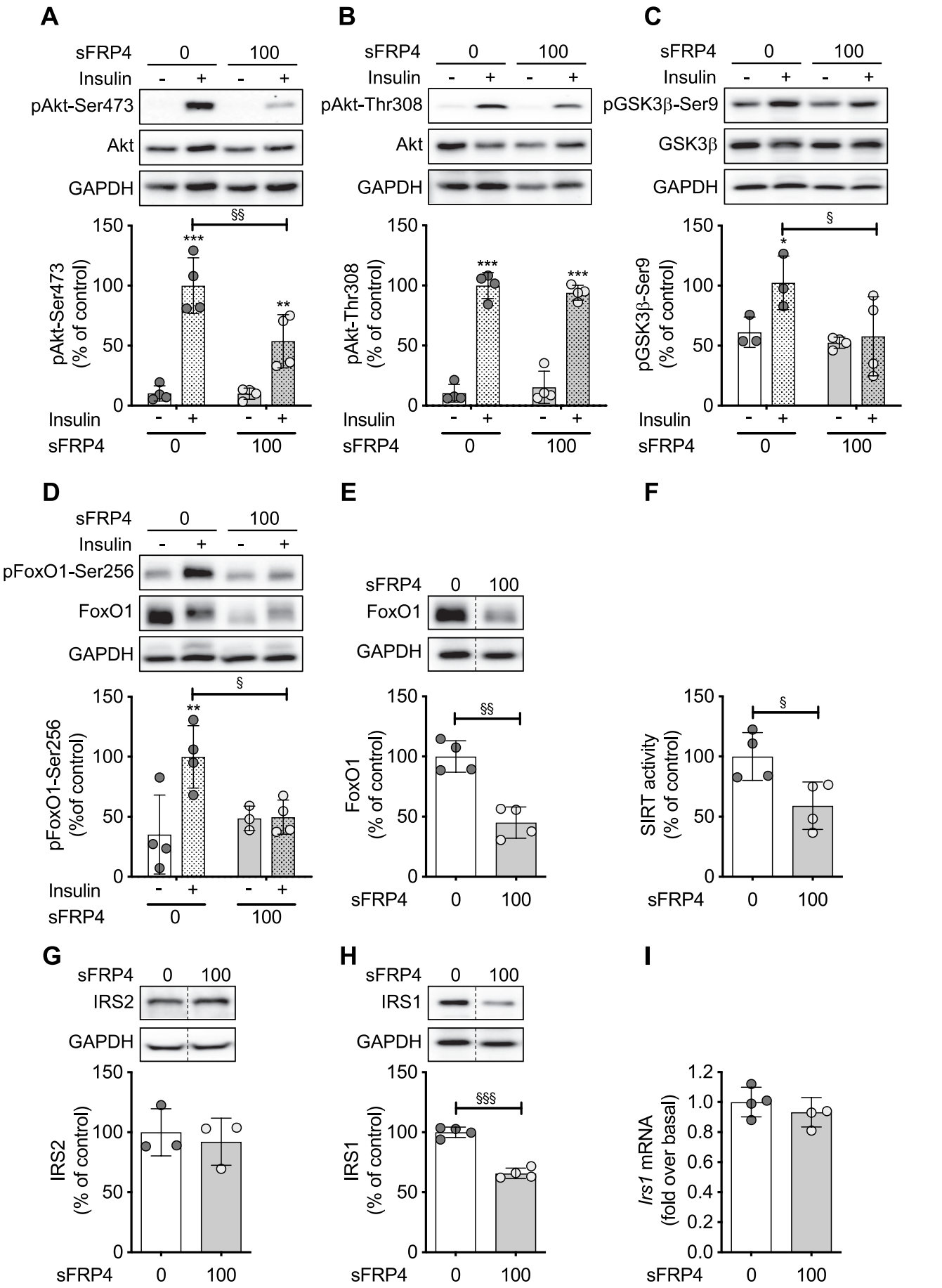

(caption on next page)

Fig. 2. sFRP4 impairs insulin signalling in primary hepatocytes from C57Bl6 mice.
Representative Western blots and graphs show the effects of 100 μg/l sFRP4 for 24 h on insulin-stimulated phosphorylation of Akt-Ser473 (A), Akt-Thr308 (B), GSK3β-Ser9 (C), and FoxO1-Ser256 (D), and the effects of sFRP4 on the protein abundances of FoxO1 (E), IRS2 (G), and IRS1 (H), sirtuin (SIRT) activity (G), and gene expression of Irs1 (I). The scattered bar graphs indicate the mean ± SD for the phosphorylation levels and abundances obtained in four independent experiments using hepatocyte preparations from different mice. The phosphorylation levels of Akt and GSK3β were corrected for the abundance of the non-phosphorylated protein and GAPDH, whereas the phosphorylation levels of FoxO1 were corrected for the abundance of GAPDH only. The values obtained in hepatocytes incubated for 10 min with 100 nmol/l insulin only (A–G) or untreated cells (H) were considered as control and set at 100% or 1. The effects of sFRP4 and insulin on phosphorylation levels were analyzed by two-way ANOVA with Sidak's correction for multiple comparisons. The effect of sFRP4 on protein abundance and *Irs1* gene expression was evaluated using a student's *t*-test. */§$p < 0.05$, **/§§$p < 0.01$ and ***$p < 0.001$; * with vs without insulin stimulation, § with vs without sFRP4 incubation.

lipogenesis in hepatocytes, which could contribute to the development of fatty liver, and the associated lipotoxic effects may include the induction of mitochondrial malfunction. Therefore, we examined the effects of sFRP4 on living primary C57Bl6 hepatocytes using Seahorse technology. As shown in supplementary Fig. 4, incubation with sFRP4 did not affect basal mitochondrial respiration, ATP production, and proton leakage in hepatocytes. Maximal respiration, spare respiratory capacity, and coupling efficiency were slightly increased by 14.4% ($p < 0.05$), 21.8% ($p < 0.05$), and 22.5% ($p < 0.01$) by sFRP4 (Supplementary Fig. 4A–F). Oxidation of ^{14}C-palmitate into CO_2, as well as ^{3}H-palmitate uptake were unaffected by sFRP4 (Supplementary Fig. 4G–H).

3.6. Effects of sFRP4 on skeletal muscle metabolism

In contrast to hepatocytes, sFRP4 did not impair the insulin-mediated phosphorylation of Akt-Ser473, Akt-Thr308, and GSK3β-Ser9 in myotubes, but the levels of phosphorylated FoxO1-Ser256 were decreased (Supplementary Fig. 5A–D). However, the FoxO1 protein levels were not reduced in myotubes exposed to sFRP4 (Supplementary Fig. 5E). Nevertheless, the incubation with sFRP4 decreased the protein abundance of IRS1 by 64% ($p < 0.01$) (Supplementary Fig. 5F). As in hepatocytes, this could not be ascribed to changes IRS1 gene expression (Supplementary Fig. 5G), but was prevented by BZ treatment prior to incubation with sFRP4 (Supplementary Fig. 6A). However, BZ did not restore the inhibition of insulin-mediated FoxO1-Ser256 phosphorylation by sFRP4 in myotubes (Supplementary Fig. 6B). sFRP4 and BZ exposure did not affect FoxO1 abundance (Supplementary Fig. 6C).

When examining mitochondrial function, we found that basal respiration was 5-fold reduced in myotubes exposed to sFRP4 ($p < 0.001$) (Fig. 5A). Also, ATP production, proton leak and coupling efficiency were reduced by 9.7- ($p < 0.01$), 2.7- ($p < 0.05$) and 1.8-fold ($p < 0.01$) upon sFRP4 incubation (Fig. 5D–F). However, maximal respiration or spare respiratory capacity were not affected by sFRP4 incubation of myotubes (Fig. 5B–C). The addition of palmitate prior to the analysis of mitochondrial function increased basal respiration, maximal respiration, ATP-production and proton leak by 1.4- ($p < 0.001$), 1.4- ($p < 0.001$), 1.3- ($p < 0.01$), and 1.5-fold ($p < 0.01$), respectively (Fig. 5A–F). The incubation with sFRP4 lowered the palmitate-induced increases in basal respiration and proton leak by 25% ($p < 0.05$) and 38% ($p < 0.05$) (Fig. 5A, E), respectively, whereas sFRP4 had no effect on palmitate-induced maximal respiration, spare respiratory capacity, ATP production, and coupling efficiency (Fig. 5B–D, F). Conventional fatty acid oxidation assays confirmed that sFRP4 does not affect the oxidation of ^{14}C-palmitate to CO_2 (Fig. 5G).

The ECAR's recorded during the Seahorse-based analysis of mitochondrial function in myotubes showed that sFRP4 induces a shift toward a more glycolytic phenotype (Supplementary Fig. 7). In a glycolytic rate assay, sFRP4 promoted a 3.2-fold increase in the ratio between glycolytic and mitochondrial oxidative capacity ($p < 0.001$) (Fig. 5H). Furthermore, sFRP4 increased the basal proton efflux rate and basal glycolysis 2.5- ($p < 0.01$) and 2.8-fold ($p < 0.001$), respectively (Fig. 5I–J). Accordingly, the percentage of protons derived from glycolysis was increased from 81.4% to 91.3% upon sFRP4 treatment of myotubes (Fig. 5K). Also, compensatory glycolysis, examined after injection with rotenone/antimycin A, was increased by 2.2-fold ($p < 0.05$) in sFRP4-treated myotubes (Fig. 5L).

3.7. Effects of sFRP4 action in hepatocytes from a mouse model with lipodystrophy

Finally, we examined whether the effects of sFRP4 are affected by massive lipid overload in hepatocytes. Therefore, we used hepatocytes isolated from the well-described aP2-SREBP-1c mouse model that is characterized by a complete loss of adipose tissue and fatty liver with systemic insulin resistance without any dietary intervention (Supplementary Table 3) [13]. Furthermore, the hepatocytes isolated from these mice are characterized by the accumulation of large lipid droplets [13]. Circulating sFRP4 levels in aP2-SREBP-1c mice were lower versus C57Bl6 control mice (aP2-SREBP-1c: 36.38 (33.24–39.51) μg/l versus C57Bl6: 44.95 (40.29–49.61) μg/l, $p = 0.002$), thereby confirming VAT as source for sFRP4 release (Supplementary Fig. 8A). Gene expression of sFRP4 in m. gastrocnemius, liver, and pancreas was comparable between the two mouse strains (Supplementary Fig. 8B).

Hepatocytes from aP2-SREBP-1c mice showed a higher DNL rate compared to C57Bl6 (Fig. 6A vs 4E), which was not significantly affected by insulin treatment or pre-incubation with sFRP4 (Fig. 6A).

Mitochondrial function in aP2-SREBP-1c hepatocytes was comparable to C57Bl6 hepatocytes, and was not affected by sFRP4 (Supplementary Fig. 9A). Furthermore, sFRP4 did not interfere with palmitate uptake and oxidation (Supplementary Fig. 9G and H).

In the absence of statistically significant effects on IRS1 protein abundance in aP2-SREBP-1c hepatocytes (Fig. 6B), sFRP4 severely impaired the insulin-mediated phosphorylation of components of the Akt signalling pathway. In aP2-SREBP-1c hepatocytes, sFRP4 impaired insulin-mediated Akt-Ser473 phosphorylation by 55% ($p < 0.001$) versus 46% in C57Bl6 hepatocytes (Figs. 6C and 2A), and completely abrogated insulin-mediated Akt-Thr308 phosphorylation in contrast to C57Bl6 hepatocytes (Fig. 6D). As in C57Bl6 hepatocytes, sFRP4 abrogated the induction of GSK3β-Ser9 phosphorylation (Fig. 6E). Furthermore, sFRP4 reduced FoxO1 abundance when normalized to GAPDH by 83% (Fig. 6F). Consequently, the absolute levels of FoxO1-Ser256 phosphorylation were lower in aP2-SREBP-1c hepatocytes that were exposed sFRP4 versus untreated cells (Fig. 6G). However, FoxO1-Ser256 phosphorylation levels when normalized to FoxO1 protein level were increased by insulin (Fig. 6H).

4. Discussion

Here we showed that sFRP4 expression is increased in VAT from obese men and associated with insulin resistance and triglycerides. In vitro studies on hepatocytes showed that sFRP4 disturbed insulin action by reducing the protein abundances of IRS1 and FoxO1 and blunting Akt signalling pathway. The latter effect was even stronger in hepatocytes isolated from aP2-SREBP-1c mice with lipodystrophy and ectopic hepatic lipid accumulation. The inhibition of insulin action in hepatocytes was selective since insulin-stimulated DNL was not impaired by sFRP4 in hepatocytes isolated from both C57Bl6 and aP2-SREBP1c mice. Furthermore, we showed that sFRP4 strongly increased basal glycolysis in myotubes, which may aggravate hepatic steatosis and

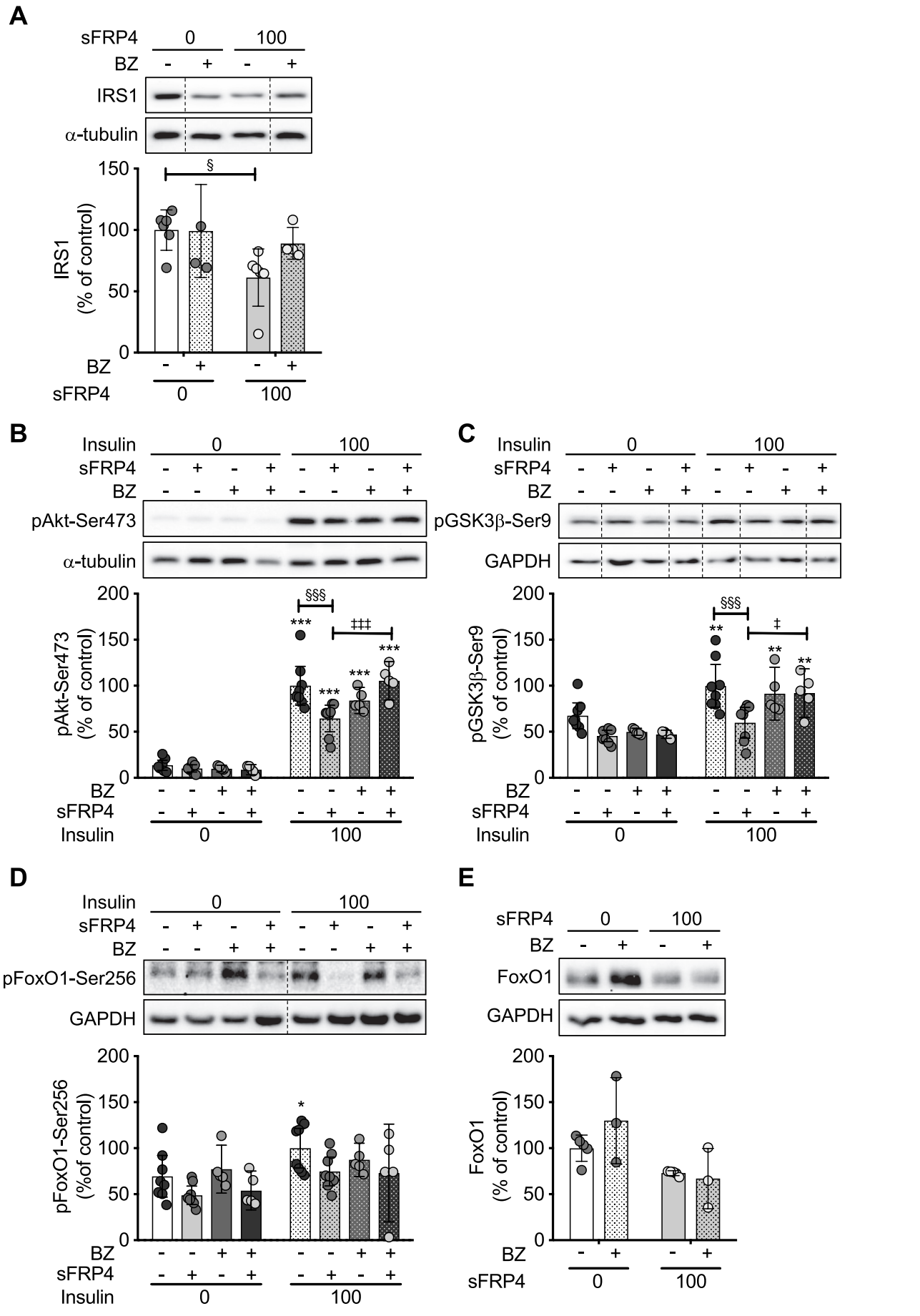

(caption on next page)

Fig. 3. Effect of the proteasome inhibitor bortezomib on sFRP4 action in hepatocytes.
The graphs and representative Western blots show the effects of sFRP4 with or without bortezomib (BZ) pretreatment on IRS1 protein abundance (A), on the insulin-stimulated phosphorylation of Akt-Ser473 (B), GSK3β-Ser9 (C), and FoxO1-Ser256 (D), and the protein abundance of FoxO1 (E). The scattered bar graphs indicate the mean ± SD for the phosphorylation levels and abundances obtained in five independent experiments using hepatocyte preparations from different mice. The phosphorylation levels were corrected for the abundance of GAPDH. The values obtained in hepatocytes incubated for 10 min with 100 nmol/l insulin only were considered as control and set at 100%. The effects of BZ, sFRP4 and insulin on phosphorylation levels and protein abundances were analyzed by ANOVA with Sidak's correction for multiple comparisons. */§/‡$p < 0.05$, **$p < 0.01$ and ***/‡‡‡$p < 0.001$; * with vs without insulin stimulation, § with vs without sFRP4 incubation, ‡ with vs without BZ incubation.

associated insulin resistance.

The in vitro data are corroborated by findings in clinical studies on normal-weight to slightly overweight participants, which showed that systemic sFRP4 interfered with insulin secretion, associated with measures of insulin resistance, such as HOMA-IR [8,22], clamp-measured insulin sensitivity [23], and the oGTT-based insulin sensitivity index [9], as well as triglycerides [8,11]. Although circulating sFRP4 levels displayed weak associations with BMI and triglycerides, an increase in patients with type 2 diabetes as observed in previous studies [8,11,23] was not observed in our cohort enrolling normal-weight men and men with extreme obesity. A potential cause for this discrepancy may be the ethnical background of the study population. Two of the afore-mentioned studies reporting increased sFRP4 levels were conducted on normal-weight Chinese [22] or Asian-Indian [8] patients with type 2 diabetes, whereas the third study reports on findings collected in a rather small group (n = 12) of slightly overweight probands of both Caucasian and African-American background [23]. Besides, one should note that our study was conducted on men. Because the circulating sFRP4 levels are comparable between Chinese men and women [22], and adjusting for sex did not impair the reported relations between circulating sFRP4 and insulin resistance in two reports [8,9], it seems unlikely that the sole inclusion of male probands could affect the interpretation of the data. In line with another study [24], we confirmed that the expression of sFRP4 in adipose tissue is increased in obesity, and that the expression levels associated with BMI, insulin resistance, insulin secretion and triglycerides. This observation and the previously reported increase in sFRP4 expression in adipose tissue in patients with NAFLD [10] strongly support the idea that the liver is an important target tissue for sFRP4 action.

A key finding of this study represents the detrimental effect of sFRP4 on hepatic insulin action. The in vitro experiments showed that sFRP4 disturbed insulin signalling at multiple levels. One level may involve IRS1 protein abundance reduction in metabolically healthy hepatocytes and myotubes. One may ascribe the reduction in IRS1 abundance to activation of the proteasome. Inhibition of proteasome activity prevented the sFRP4-mediated reduction in IRS1 protein abundance and

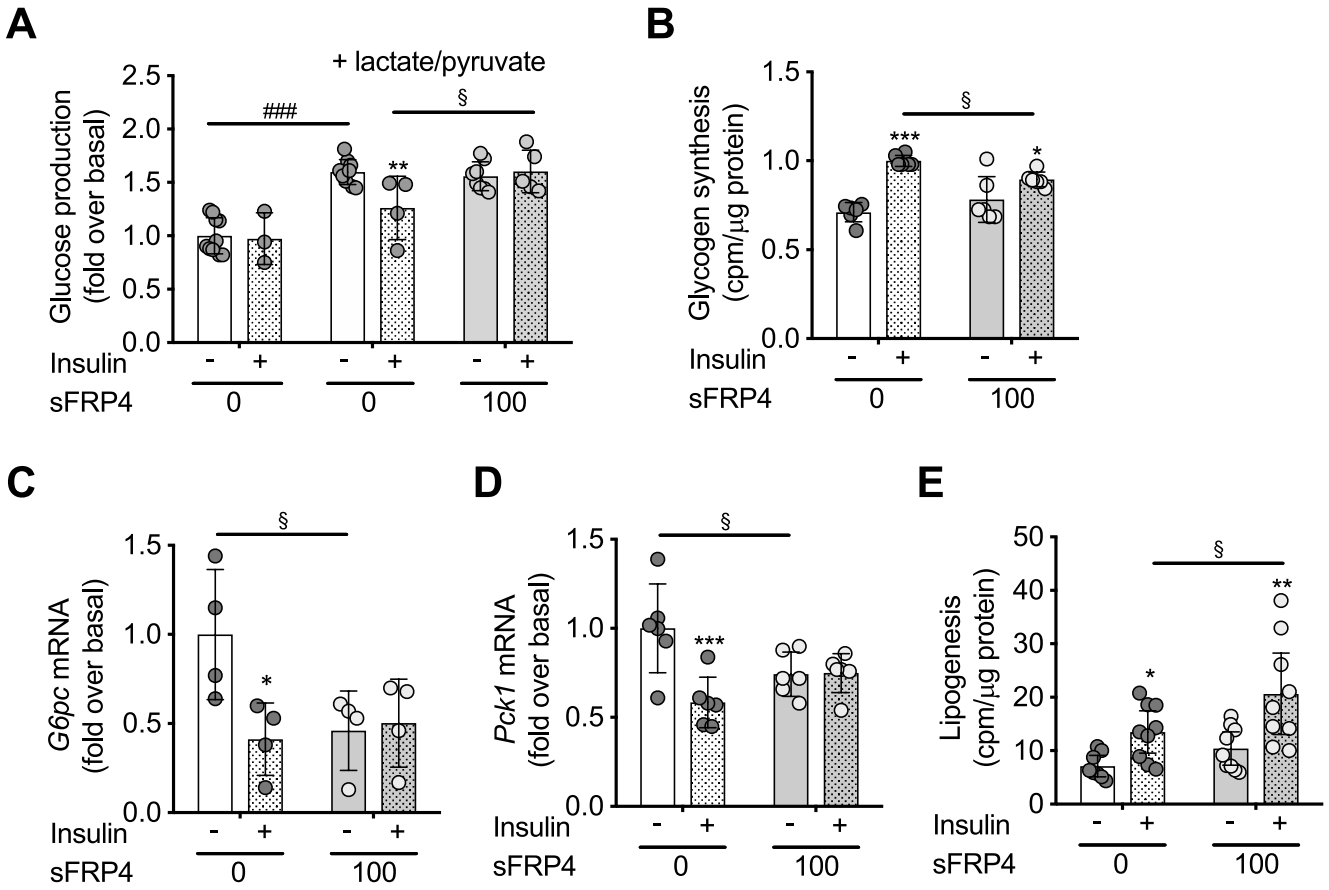

Fig. 4. Effect of sFRP4 on glucose metabolism and lipogenesis in primary hepatocytes from C57Bl6 mice.
Primary murine hepatocytes were incubated with sFRP4 for 24 h or kept untreated prior to the analysis of glucose production (n = 4) (A), glycogen synthesis (n = 6) (B), gene expression of *G6pc* (n = 4) (C) and *Pck1* (n = 4) (D), and lipogenesis (n = 5) (E). The values obtained for untreated cells in the glucose production experiments (A, C, D) were considered as control and set at 1. The scattered bar graphs depict the data as mean ± SD. The effects of sFRP4 and insulin were analyzed by two-way ANOVA with Sidak's correction for multiple comparisons. */§$p < 0.05$ and ***/§§§$p < 0.001$; * with vs without insulin stimulation, § with vs without sFRP4 incubation.

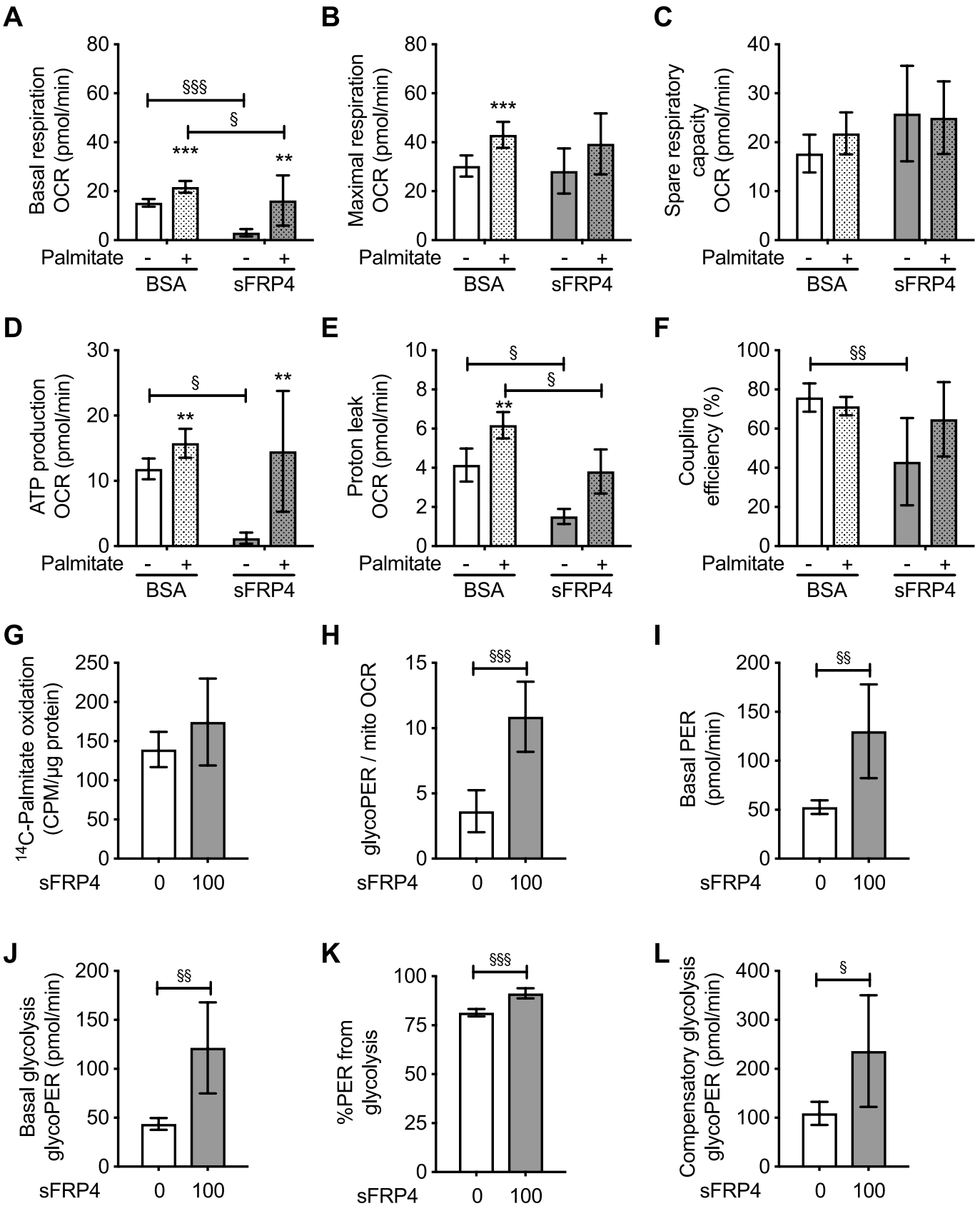

(caption on next page)

Fig. 5. Effect of sFRP4 on mitochondrial function, palmitate oxidation and glycolysis in primary human myotubes.
(A–F) Determinants of mitochondrial function in primary human myotubes. The bar graphs depict basal respiration (A), maximal respiration (B), spare respiratory capacity (C), ATP production (D), proton leak (E), and coupling efficiency (F) as calculated from a Seahorse mito-stress test in primary human skeletal muscle cells that were exposed to sFRP4 for 24 h or kept untreated. The mito-stress assay was performed after the addition of BSA or palmitate, which were added immediately before the start of the Seahorse analysis. The data are the mean ± SD of at least 4 independent experiments using primary skeletal muscle cells from 3 different donors. (G) Effect of sFRP4 on the ^{14}C-palmitate oxidation in primary human myotubes that were incubated with sFRP4 or not. Data are the mean ± SD for the oxidation of ^{14}C-palmitate of 6 independent experiments. (H–L) Determinants of glycolytic function in primary human myotubes. The bar graphs depict the ratio between glycolytic PER and baseline mitochondrial OCR (H), basal PER (I), basal glycolysis (J), %PER from glycolysis (K), and compensatory glycolysis (L) as calculated from a Seahorse glycolytic rate assay in primary human skeletal muscle cells that were exposed to sFRP4 for 24 h or kept untreated. The data are the mean ± SD of five independent experiments using primary skeletal muscle cells from 3 different donors. */§$p < 0.05$, **/§§$p < 0.01$ and ***/§§§$p < 0.001$; * with vs without palmitate incubation, § with vs without sFRP4 incubation.

the inhibition of the phosphorylation of Akt-Ser473 and GSK3β-Ser9 in hepatocytes. This suggests that the amount of IRS1 is critical for activation of the Akt/GSK3β arm of the insulin signalling cascade in hepatocytes. However, in myotubes there was no inhibition of insulin-mediated phosphorylation of Akt and GSK3β by sFRP4 despite reductions in IRS1 protein abundance. It remains to be investigated what underlies the tissue-specific inhibition of insulin action by sFRP4. sFRP4 is a modulator of the activity of the canonical Wnt signalling pathway, which promotes the stabilization of β-catenin and stimulation of gene expression through interaction with the T-cell factor transcription factors [25]. Activation of Wnt signalling is initiated by binding of the Wnt-ligands to the frizzled receptors, whereas inactivation is regulated by the binding of the sFRP's, including sFRP4 to the Wnt-ligands [25]. Since at least 19 different Wnt-ligands have been identified that can bind to at least 10 different Frizzled receptors [25], one may speculate that differences in the tissue distribution of Wnt-ligands and Frizzled receptors underlie the differences in sFRP4 signalling between hepatocytes and myotubes.

Proteasome inhibition did not prevent the sFRP4-mediated reduction in FoxO1 protein abundance in hepatocytes. This observation indicates an additional level via which sFRP4 disturbs insulin action. FoxO1 regulates gluconeogenic gene expression and activates hepatic glucose production in fasting periods, which can be suppressed depending on insulin by Akt activation [26]. In response to sFRP4, both the protein abundance and insulin-mediated phosphorylation of FoxO1 were reduced. Consequently, when sFRP4 treatment is combined with insulin stimulation in C57Bl6 hepatocytes, the absolute phosphorylation levels of FoxO1 are not further increased, and one may expect that the already lower expression of FoxO1-regulated genes is not further suppressed. Independent from phosphorylation, the activity of FoxO1 is additionally controlled by acetylation. Increases in CBP/p300-mediated FoxO1-acetylation, reduces its affinity to the DNA. On the other hand, deacetylation of FoxO1, as mediated by the SIRT family of deacetylases, increases the DNA-binding affinity of FoxO1. Thus, the sFRP4-mediated reduction in SIRT activity in hepatocytes may further reduce FoxO1 activity. One may assume that the lower expression of the FoxO1-regulated genes *G6pc* and *Pck1* in sFRP4-treated C57Bl6 hepatocytes can be ascribed to reductions in FoxO1 activity. The reduction in FoxO1 activity may also indicate an attempt to compensate for sFRP4 interference with insulin signalling at FoxO1. Constitutively active hepatic FoxO1 has been associated with impaired fasting glucose, hyperinsulinemia and increased triglyceride levels and steatosis in mice. Furthermore, upon liver-specific deletion of FoxO1, gluconeogenesis was reduced and hyperglycemia improved in obese mice [27,28]. Mice with liver-specific loss of either the insulin receptor, Akt or IRS-1/IRS-2 showed increased FoxO1-mediated hepatic glucose production along with severe insulin resistance and glucose intolerance, while if there was simultaneous ablation of FoxO1 in the liver, these metabolic disorders were restored, leading to suppression of hepatic glucose production in response to insulin and improved glucose tolerance [29,30]. These studies proposed an additional IR-, IRS- and Akt-independent mechanism through which FoxO1 regulates hepatic glucose production [30].

Importantly, the stimulation of DNL by insulin was not inhibited by sFRP4. Rather, sFRP4 even enhanced the stimulation of DNL in hepatocytes. The sFRP4-mediated decrease in FoxO1 protein expression may contribute to this enhanced lipogenesis, since studies on isolated hepatocytes demonstrated that inhibition of FoxO1 as such is sufficient to drive lipogenesis [31]. However, one should also note that the selective inhibition of the activation of Akt signalling by insulin in concert with the stimulation of lipogenesis closely resembles the paradox of selective hepatic insulin resistance in type 2 diabetes as proposed by Brown and Goldstein [32]. Here, insulin signalling via the Akt/FoxO1-pathway is impaired. This results in impaired suppression of hepatic gluconeogenesis by insulin, but promotes the other main action of insulin in the liver, namely the stimulation of DNL via the transcription factor SREBP-1c [32]. Increased DNL can result in hepatic lipid accumulation, which on its turn is highly associated with insulin resistance [13,17].

Here, we also examined the effects of sFRP4 on insulin action in hepatocytes from lipodystrophic aP2-SREBP-1c mice. In humans, lipodystrophy leads to excessive ectopic storage of fat in the liver associated with increased liver DNL, severe hepatic insulin resistance, dyslipidaemia, hyperglycaemia, hypertriglyceridemia, hyperinsulinemia and NAFLD [33–35]. The aP2-SREBP-1c mice are characterized by massive hepatic lipid accumulation due to the complete lack of adipose tissue and thus the absence of adipose tissue lipid storage capacity and systemic insulin resistance associated with reduced insulin action but increased hepatic lipogenesis [12,13,36]. Accordingly, we found that DNL in lipodystrophic mice was higher than in C57Bl6, but neither insulin nor sFRP4 further increased DNL in aP2-SREBP1c hepatocytes as seen in hepatocytes of metabolic healthy C57Bl6 mice. In the absence of an effect on lipid uptake and oxidation, sFRP4 incubation caused a more severe inhibition of the insulin signalling pathway to Akt in aP2-SREBP-1c compared to C57Bl6 hepatocytes. This suggests that hepatic lipid accumulation aggravates the detrimental effects of sFRP4 on hepatic insulin sensitivity.

Apart from the effects of sFRP4 on lipogenesis found in hepatocytes from metabolically healthy C57Bl6 hepatocytes mice, also indirect effects of sFRP4 may contribute to hepatic lipid accumulation. In myotubes, sFRP4 caused a marked increase in glycolysis. The resulting lactate, using the Cori cycle, may be converted to glucose in the liver, which on its turn can be oxidized, stored as glycogen or converted into lipids. The in vitro studies showed that sFRP4 did not impair hepatocyte mitochondrial function, and that it inhibits the stimulation of glycogen synthesis by insulin. Therefore, one may speculate that enhanced glycolysis in skeletal muscle may contribute to enhanced lipid accumulation by enhancing lipogenesis. However, further in vivo studies are needed to support this.

The increased *sFRP4* expression in subjects with obesity or type 2 diabetes, which was also reported by others [24,37], may suggest that sFRP4 acts as an adipokine. Accordingly, the analysis of plasma samples from lipodystrophic aP2-SREBP-1c mice lacking adipose tissue showed a decrease in circulating sFRP4 levels compared to C57Bl6 mice. However, the data also showed that adipose tissue is not the only source for systemic sFRP4. This confirmed other reports that sFRP4 is also expressed and/or secreted in other tissues, such as the liver, the pancreas and skeletal muscle [9,38–41]. However, it remains to be investigated whether a deregulated expression of sFRP4 in the context of

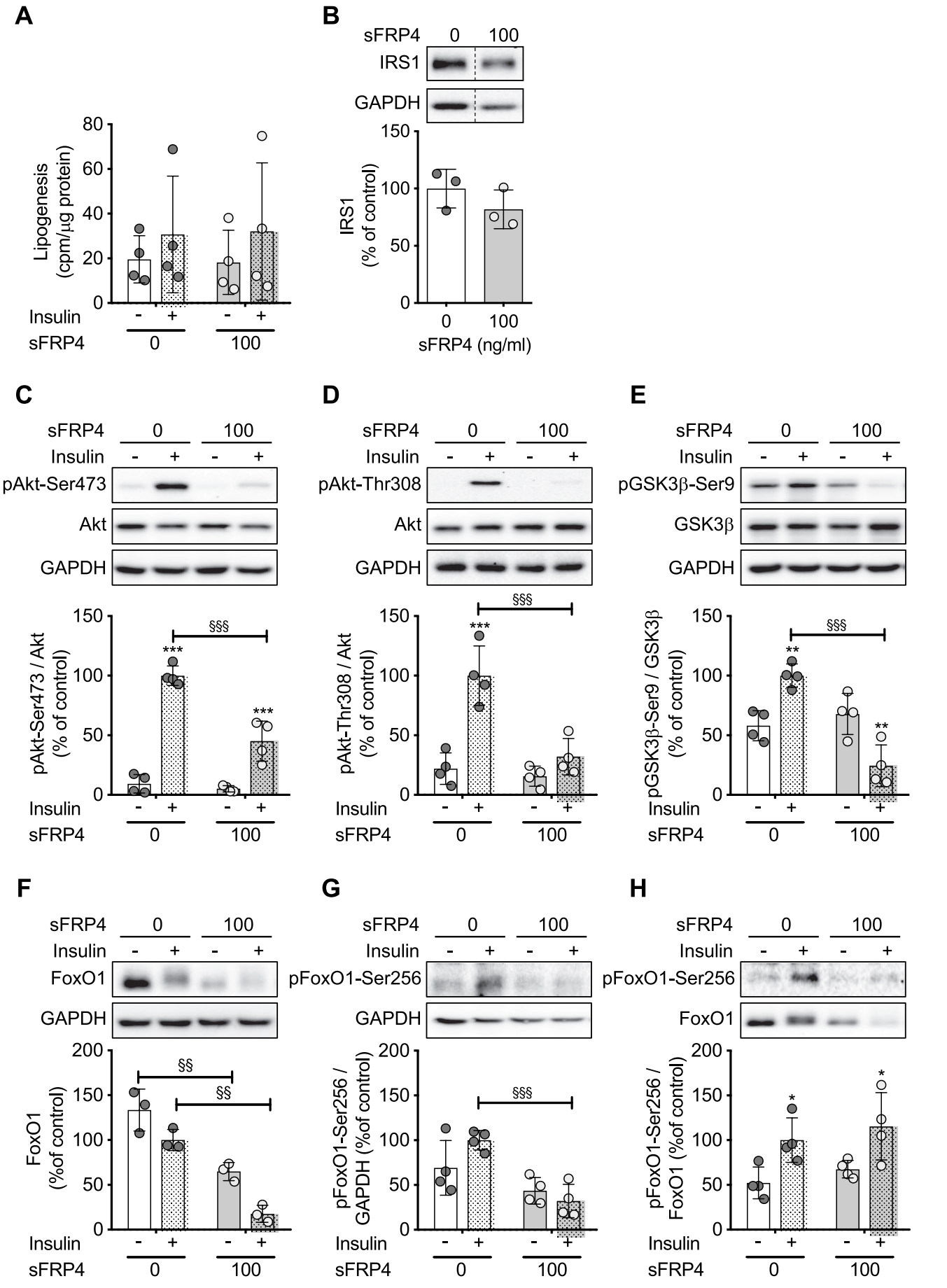

(caption on next page)

Fig. 6. Effect of sFRP4 on lipogenesis and insulin action in hepatocytes from aP2-SREBP-1c mice.
Primary murine hepatocytes isolated from aP2-SREBP-1c mice were incubated with sFRP4 for 24 h or kept untreated prior to the analysis of lipogenesis (n = 4) (A) or phosphorylation and protein abundance of the insulin signalling system (B–H). Representative Western blots and graphs show the effects of sFRP4 on the protein abundance of IRS1 (B) FoxO1 (F), and the insulin-stimulated phosphorylation of Akt-Ser473 (C), Akt-Thr308 (D), GSK3β-Ser9 (E), and FoxO1-Ser256 (G,H). The scattered bar graphs indicate the mean ± SD for the phosphorylation levels and abundances obtained in four independent experiments using hepatocyte preparations from different mice. The phosphorylation levels were corrected for the abundance of the non-phosphorylated protein and GAPDH. The values obtained in hepatocytes incubated for 10 min with 100 nmol/l insulin only were considered as control and set at 100%. The effects of sFRP4 and insulin on phosphorylation levels were analyzed by two-way ANOVA with Sidak's correction for multiple comparisons. The effect of sFRP4 on protein abundance was evaluated using a Student's t-test. *$p < 0.05$, **/§§$p < 0.01$ and ***$p < 0.001$; * with vs without insulin stimulation, § with vs without sFRP4 incubation.

obesity and type 2 diabetes is also found in these non-adipose tissues. At least in aP2-SREBP-1c mice, we found no upregulation in non-adipose *sFRP4* expression versus the C57Bl6 model.

Collectively, we show an association between *sFRP4* expression in adipose tissue with insulin sensitivity and triglyceride levels in human. In vitro studies on hepatocytes showed that sFRP4 selectively inhibits the insulin signalling pathway regulating glucose metabolism, while enhancing the stimulation of DNL. The latter may be further enhanced by increased glycolysis in sFRP4-treated myotubes. Finally, as proof of principle in hepatocytes isolated from a lipodystrophic mouse model with hepatic lipid accumulation, we found that sFRP4 further aggravates insulin action. Based on these data and the notion that sFRP4 levels are increased already before the onset of type 2 diabetes [9], sFRP4 may be an attractive target to mitigate pathophysiological changes that occur during the development of type 2 diabetes and fatty liver disease.

Supplementary data to this article can be found online at https://doi.org/10.1016/j.bbadis.2019.07.008.

Transparency document

The Transparency document associated with this article can be found, in online version.

Author contributions

T.H., P.F., D.B., D.H., H.T., performed experiments and researched the data. F.V., B.L., Y.N., conducted the clinical study. T.H., B.K., D.M.O., J.K. analyzed the data, and wrote the paper. J.K., B.K., D.M.O. designed the study. D.M.-W., H.A.-H., contributed to data interpretation and discussion. J.K. is the guarantor of this work, had full access to all the data, and takes full responsibility for the integrity of the data and the accuracy of the data analysis. All authors have seen and approved the final version of the manuscript.

Declaration of Competing Interest

The authors declare that there is no duality of interest associated with this study.

Acknowledgements

The work was supported by the German Diabetes Centre (DDZ), which is funded by the German Federal Ministry of Health and the Ministry of Innovation, Science, Research and Technology of the state North Rhine-Westphalia. This study was supported in part by a grant from the German Federal Ministry of Education and Research (BMBF) to the German Center for Diabetes Research (DZD e.V.).

References

[1] R.H. Unger, Lipid overload and overflow: metabolic trauma and the metabolic syndrome, Trends Endocrinol. Metab. 14 (2003) 398–403.
[2] B. Knebel, S. Goeddeke, G. Poschmann, D.F. Markgraf, S. Jacob, U. Nitzgen, W. Passlack, C. Preuss, H.D. Dicken, K. Stuhler, S. Hartwig, S. Lehr, J. Kotzka, Novel insights into the Adipokinome of obese and obese/diabetic mouse models, Int. J. Mol. Sci. 18 (2017), https://doi.org/10.3390/ijms18091928.
[3] G. Marchesini, M. Brizi, G. Bianchi, S. Tomassetti, E. Bugianesi, M. Lenzi, A.J. McCullough, S. Natale, G. Forlani, N. Melchionda, Nonalcoholic fatty liver disease: a feature of the metabolic syndrome, Diabetes. 50 (2001) 1844–1850.
[4] K.L. Donnelly, C.I. Smith, S.J. Schwarzenberg, J. Jessurun, M.D. Boldt, E.J. Parks, Sources of fatty acids stored in liver and secreted via lipoproteins in patients with nonalcoholic fatty liver disease, J. Clin. Invest. 115 (2005) 1343–1351, https://doi.org/10.1172/JCI23621.
[5] A.L. Birkenfeld, G.I. Shulman, Nonalcoholic fatty liver disease, hepatic insulin resistance, and type 2 diabetes, Hepatology. 59 (2014) 713–723, https://doi.org/10.1002/hep.26672.
[6] E. Fabbrini, S. Sullivan, S. Klein, Obesity and nonalcoholic fatty liver disease: biochemical, metabolic, and clinical implications, Hepatology. 51 (2010) 679–689, https://doi.org/10.1002/hep.23280.
[7] D.E. Kleiner, E.M. Brunt, M. Van Natta, C. Behling, M.J. Contos, O.W. Cummings, L.D. Ferrell, Y.C. Liu, M.S. Torbenson, A. Unalp-Arida, M. Yeh, A.J. McCullough, A.J. Sanyal, N. Nonalcoholic Steatohepatitis Clinical Research, Design and validation of a histological scoring system for nonalcoholic fatty liver disease, Hepatology. 41 (2005) 1313–1321, https://doi.org/10.1002/hep.20701.
[8] K. Anand, S. Vidyasagar, I. Lasrado, G.K. Pandey, A. Amutha, H. Ranjani, R. Mohan Anjana, V. Mohan, K. Gokulakrishnan, Secreted frizzled-related protein 4 (SFRP4): a novel biomarker of beta-cell dysfunction and insulin resistance in individuals with prediabetes and type 2 diabetes, Diabetes Care 39 (2016) e147–e148, https://doi.org/10.2337/dc16-0756.
[9] T. Mahdi, S. Hanzelmann, A. Salehi, S.J. Muhammed, T.M. Reinbothe, Y. Tang, A.S. Axelsson, Y. Zhou, X. Jing, P. Almgren, U. Krus, J. Taneera, A.M. Blom, V. Lyssenko, J.L. Esguerra, O. Hansson, L. Eliasson, J. Derry, E. Zhang, C.B. Wollheim, L. Groop, E. Renstrom, A.H. Rosengren, Secreted frizzled-related protein 4 reduces insulin secretion and is overexpressed in type 2 diabetes, Cell Metab. 16 (2012) 625–633, https://doi.org/10.1016/j.cmet.2012.10.009.
[10] M. Bekaert, D.M. Ouwens, T. Horbelt, F. Van de Velde, P. Fahlbusch, D. Herzfeld de Wiza, Y. Van Nieuwenhove, P. Calders, M. Praet, A. Hoorens, A. Geerts, X. Verhelst, J.M. Kaufman, B. Lapauw, Reduced expression of chemerin in visceral adipose tissue associates with hepatic steatosis in patients with obesity, Obesity (Silver Spring) 24 (2016) 2544–2552, https://doi.org/10.1002/oby.21674.
[11] J.M. Brix, E.C. Krzizek, C. Hoebaus, B. Ludvik, G. Schernthaner, G.H. Schernthaner, Secreted frizzled-related protein 4 (SFRP4) is elevated in patients with diabetes mellitus, Horm. Metab. Res. 48 (2016) 345–348, https://doi.org/10.1055/s-0041-111698.
[12] I. Shimomura, R.E. Hammer, J.A. Richardson, S. Ikemoto, Y. Bashmakov, J.L. Goldstein, M.S. Brown, Insulin resistance and diabetes mellitus in transgenic mice expressing nuclear SREBP-1c in adipose tissue: model for congenital generalized lipodystrophy, Genes Dev. 12 (1998) 3182–3194.
[13] T. Jelenik, K. Kaul, G. Sequaris, U. Flogel, E. Phielix, J. Kotzka, B. Knebel, P. Fahlbusch, T. Horbelt, S. Lehr, A.L. Reinbeck, D. Muller-Wieland, I. Esposito, G.I. Shulman, J. Szendroedi, M. Roden, Mechanisms of insulin resistance in primary and secondary nonalcoholic fatty liver, Diabetes. 66 (2017) 2241–2253, https://doi.org/10.2337/db16-1147.
[14] T. Horbelt, C. Tacke, M. Markova, D. Herzfeld de Wiza, F. Van de Velde, M. Bekaert, Y. Van Nieuwenhove, S. Hornemann, M. Rodiger, N. Seebeck, E. Friedl, W. Jonas, G.H. Thoresen, O. Kuss, A. Rosenthal, V. Lange, A.F.H. Pfeiffer, A. Schurmann, B. Lapauw, N. Rudovich, O. Pivovarova, D.M. Ouwens, The novel adipokine WISP1 associates with insulin resistance and impairs insulin action in human myotubes and mouse hepatocytes, Diabetologia. (2018), https://doi.org/10.1007/s00125-018-4636-9.
[15] J.B. Ruige, M. Bekaert, B. Lapauw, T. Fiers, S. Lehr, S. Hartwig, D. Herzfeld de Wiza, M. Schiller, W. Passlack, Y. Van Nieuwenhove, P. Pattyn, C. Cuvelier, Y.E. Taes, H. Sell, J. Eckel, J.M. Kaufman, D.M. Ouwens, Sex steroid-induced changes in circulating monocyte chemoattractant protein-1 levels may contribute to metabolic dysfunction in obese men, J. Clin. Endocrinol. Metab. 97 (2012) E1187–E1191, https://doi.org/10.1210/jc.2011-3069.
[16] P. Bedossa, C. Poitou, N. Veyrie, J.L. Bouillot, A. Basdevant, V. Paradis, J. Tordjman, K. Clement, Histopathological algorithm and scoring system for evaluation of liver lesions in morbidly obese patients, Hepatology. 56 (2012) 1751–1759, https://doi.org/10.1002/hep.25889.
[17] B. Knebel, S. Hartwig, J. Haas, S. Lehr, S. Goeddeke, F. Susanto, L. Bohne, S. Jacob, C. Koellmer, U. Nitzgen, D. Muller-Wieland, J. Kotzka, Peroxisomes compensate hepatic lipid overflow in mice with fatty liver, Biochim. Biophys. Acta 1851 (2015) 965–976, https://doi.org/10.1016/j.bbalip.2015.03.003.
[18] M. Blumensatt, P. Fahlbusch, R. Hilgers, M. Bekaert, D. Herzfeld de Wiza, P. Akhyari, J.B. Ruige, D.M. Ouwens, Secretory products from epicardial adipose tissue from patients with type 2 diabetes impair mitochondrial beta-oxidation in cardiomyocytes via activation of the cardiac renin-angiotensin system and induction of miR-208a, Basic Res. Cardiol. 112 (2017) 2, https://doi.org/10.1007/

s00395-016-0591-0.
[19] N. Romero, P. Swain, A. Neilson, B.P. Dranka, Improving Quantification of Cellular Glycolytic Rate Using Agilent Seahorse XF Technology (White Paper), Agilent Technologies (Doc. No. 5991-7894EN-D4). Available from, 2017. http://seahorseinfo.agilent.com/acton/fs/blocks/showLandingPage/a/10967/p/p-00ca/t/page/fm/1.
[20] S. Goddeke, B. Knebel, P. Fahlbusch, T. Horbelt, G. Poschmann, F. van de Velde, T. Benninghoff, H. Al-Hasani, S. Jacob, Y. Van Nieuwenhove, B. Lapauw, S. Lehr, D.M. Ouwens, J. Kotzka, CDH13 abundance interferes with adipocyte differentiation and is a novel biomarker for adipose tissue health, Int. J. Obes. 42 (2018) 1039–1050, https://doi.org/10.1038/s41366-018-0022-4.
[21] D. Accili, K.C. Arden, FoxOs at the crossroads of cellular metabolism, differentiation, and transformation, Cell. 117 (2004) 421–426.
[22] F. Liu, H. Qu, Y. Li, Q. Tang, Z. Yang, H. Wang, H. Deng, Relationship between serum secreted frizzled-related protein 4 levels and the first-phase of glucose-stimulated insulin secretion in individuals with different glucose tolerance, Endocr. J. 62 (2015) 733–740, https://doi.org/10.1507/endocrj.EJ15-0212.
[23] G. Garufi, A.A. Seyhan, M. Pasarica, Elevated secreted frizzled-related protein 4 in obesity: a potential role in adipose tissue dysfunction, Obesity (Silver Spring) 23 (2015) 24–27, https://doi.org/10.1002/oby.20915.
[24] A. Ehrlund, N. Mejhert, S. Lorente-Cebrian, G. Astrom, I. Dahlman, J. Laurencikiene, M. Ryden, Characterization of the Wnt inhibitors secreted frizzled-related proteins (SFRPs) in human adipose tissue, J. Clin. Endocrinol. Metab. 98 (2013) E503–E508, https://doi.org/10.1210/jc.2012-3416.
[25] H. Clevers, R. Nusse, Wnt/beta-catenin signaling and disease, Cell. 149 (2012) 1192–1205, https://doi.org/10.1016/j.cell.2012.05.012.
[26] M. Matsumoto, S. Han, T. Kitamura, D. Accili, Dual role of transcription factor FoxO1 in controlling hepatic insulin sensitivity and lipid metabolism, J. Clin. Invest. 116 (2006) 2464–2472, https://doi.org/10.1172/JCI27047.
[27] J. Altomonte, A. Richter, S. Harbaran, J. Suriawinata, J. Nakae, S.N. Thung, M. Meseck, D. Accili, H. Dong, Inhibition of Foxo1 function is associated with improved fasting glycemia in diabetic mice, Am. J. Physiol. Endocrinol. Metab. 285 (2003) E718–E728, https://doi.org/10.1152/ajpendo.00156.2003.
[28] I. O'Sullivan, W. Zhang, D.H. Wasserman, C.W. Liew, J. Liu, J. Paik, R.A. DePinho, D.B. Stolz, C.R. Kahn, M.W. Schwartz, T.G. Unterman, FoxO1 integrates direct and indirect effects of insulin on hepatic glucose production and glucose utilization, Nat. Commun. 6 (2015) 7079, https://doi.org/10.1038/ncomms8079.
[29] X.C. Dong, FOXO transcription factors in non-alcoholic fatty liver disease, Liver Res. 1 (2017) 168–173, https://doi.org/10.1016/j.livres.2017.11.004.
[30] P.M. Titchenell, Q. Chu, B.R. Monks, M.J. Birnbaum, Hepatic insulin signalling is dispensable for suppression of glucose output by insulin in vivo, Nat. Commun. 6 (2015) 7078, https://doi.org/10.1038/ncomms8078.
[31] P.M. Titchenell, W.J. Quinn, M. Lu, Q. Chu, W. Lu, C. Li, H. Chen, B.R. Monks, J. Chen, J.D. Rabinowitz, M.J. Birnbaum, Direct hepatocyte insulin signaling is required for lipogenesis but is dispensable for the suppression of glucose production, Cell Metab. 23 (2016) 1154–1166, https://doi.org/10.1016/j.cmet.2016.04.022.
[32] M.S. Brown, J.L. Goldstein, Selective versus total insulin resistance: a pathogenic paradox, Cell Metab. 7 (2008) 95–96, https://doi.org/10.1016/j.cmet.2007.12.009.
[33] A. Garg, Lipodystrophies, Am. J. Med. 108 (2000) 143–152.
[34] B. Knebel, J. Kotzka, S. Lehr, S. Hartwig, H. Avci, S. Jacob, U. Nitzgen, M. Schiller, W. Marz, M.M. Hoffmann, E. Seemanova, J. Haas, D. Muller-Wieland, A mutation in the c-fos gene associated with congenital generalized lipodystrophy, Orphanet J. Rare Dis. 8 (2013) 119, https://doi.org/10.1186/1750-1172-8-119.
[35] R.K. Semple, A. Sleigh, P.R. Murgatroyd, C.A. Adams, L. Bluck, S. Jackson, A. Vottero, D. Kanabar, V. Charlton-Menys, P. Durrington, M.A. Soos, T.A. Carpenter, D.J. Lomas, E.K. Cochran, P. Gorden, S. O'Rahilly, D.B. Savage, Postreceptor insulin resistance contributes to human dyslipidemia and hepatic steatosis, J. Clin. Invest. 119 (2009) 315–322, https://doi.org/10.1172/jci37432.
[36] I. Shimomura, Y. Bashmakov, J.D. Horton, Increased levels of nuclear SREBP-1c associated with fatty livers in two mouse models of diabetes mellitus, J. Biol. Chem. 274 (1999) 30028–30032.
[37] M. Visweswaran, L. Schiefer, F. Arfuso, R.J. Dilley, P. Newsholme, A. Dharmarajan, Wnt antagonist secreted frizzled-related protein 4 upregulates adipogenic differentiation in human adipose tissue-derived mesenchymal stem cells, PLoS One 10 (2015) e0118005, , https://doi.org/10.1371/journal.pone.0118005.
[38] S. Hartwig, S. Raschke, B. Knebel, M. Scheler, M. Irmler, W. Passlack, S. Muller, F.G. Hanisch, T. Franz, X. Li, H.D. Dicken, K. Eckardt, J. Beckers, M.H. de Angelis, C. Weigert, H.U. Haring, H. Al-Hasani, D.M. Ouwens, J. Eckel, J. Kotzka, S. Lehr, Secretome profiling of primary human skeletal muscle cells, Biochim. Biophys. Acta 1844 (2014) 1011–1017, https://doi.org/10.1016/j.bbapap.2013.08.004.
[39] J. Mastaitis, M. Eckersdorff, S. Min, Y. Xin, K. Cavino, J. Aglione, H. Okamoto, E. Na, T. Stitt, M.G. Dominguez, J.P. Schmahl, C. Lin, N.W. Gale, D.M. Valenzuela, A.J. Murphy, G.D. Yancopoulos, J. Gromada, Loss of SFRP4 alters body size, food intake, and energy expenditure in diet-induced obese male mice, Endocrinology. 156 (2015) 4502–4510, https://doi.org/10.1210/en.2015-1257.
[40] S. Pourteymour, K. Eckardt, T. Holen, T. Langleite, S. Lee, J. Jensen, K.I. Birkeland, C.A. Drevon, M. Hjorth, Global mRNA sequencing of human skeletal muscle: search for novel exercise-regulated myokines, Mol. Metab. 6 (2017) 352–365, https://doi.org/10.1016/j.molmet.2017.01.007.
[41] J. Taneera, S. Lang, A. Sharma, J. Fadista, Y. Zhou, E. Ahlqvist, A. Jonsson, V. Lyssenko, P. Vikman, O. Hansson, H. Parikh, O. Korsgren, A. Soni, U. Krus, E. Zhang, X.J. Jing, J.L. Esguerra, C.B. Wollheim, A. Salehi, A. Rosengren, E. Renstrom, L. Groop, A systems genetics approach identifies genes and pathways for type 2 diabetes in human islets, Cell Metab. 16 (2012) 122–134, https://doi.org/10.1016/j.cmet.2012.06.006.